Published in final edited form as:
Bioconjug Chem. 2008 February ; 19(2): 539–547. doi:10.1021/bc700317w.

^{111}In-labeled Lactam Bridge-cyclized Alpha-Melanocyte Stimulating Hormone Peptide Analogues for Melanoma Imaging

Yubin Miao[*,†,⊥,Φ], **Fabio Gallazzi**[‡], **Haixun Guo**[†], and **Thomas P. Quinn**[‡,§,‖]

[†]College of Pharmacy, University of New Mexico, Albuquerque, NM 87131, USA

[⊥]Cancer Research Treatment Center, University of New Mexico, Albuquerque, NM 87131, USA

[Φ]Department of Dermatology, University of New Mexico, Albuquerque, NM 87131, USA

[‡]Department of Biochemistry, University of Missouri, Columbia, MO 65211, USA

[§]Department of Radiology, University of Missouri, Columbia, MO 65211, USA

[‖]Harry S. Truman Memorial Veteran Hospital, Columbia, MO 65201, USA

Abstract

The purpose of this study was to examine the influence of the lactam bridge cyclization on melanoma targeting and biodistribution properties of the radiolabeled conjugates. Two novel lactam bridge-cyclized α-MSH peptide analogues, DOTA-CycMSH (1,4,7,10-tetraazacyclododecane-1,4,7,10-tetraacetic acid-c[Lys-Nle-Glu-His-DPhe-Arg-Trp-Gly-Arg-Pro-Val-Asp]) and DOTA-GlyGlu-CycMSH (DOTA-Gly-Glu-c[Lys-Nle-Glu-His-DPhe-Arg-Trp-Gly-Arg-Pro-Val-Asp]), were synthesized and radiolabeled with ^{111}In. The internalization and efflux of ^{111}In-labeled CycMSH peptides were examined in B16/F1 melanoma cells. The melanoma targeting properties, pharmacokinetics and SPECT/CT imaging of ^{111}In-labeled CycMSH peptides were determined in B16/F1 melanoma-bearing C57 mice. Both ^{111}In-DOTA-CycMSH and ^{111}In-DOTA-GlyGlu-CycMSH exhibited fast internalization and extended retention in B16/F1 cells. The tumor uptake values of ^{111}In-DOTA-CycMSH and ^{111}In-DOTA-GlyGlu-CycMSH were 9.53±1.41 %injected dose/gram (%ID/g) and 10.40±1.40 %ID/g at 2 h post-injection, respectively. Flank melanoma tumors were clearly visualized with ^{111}In-DOTA-CycMSH and ^{111}In-DOTA-GlyGlu-CycMSH by SPECT/CT images at 2 h post-injection. Whole-body clearance of the peptides was fast, with greater than 90% of the radioactivities cleared through urinary system by 2 h post-injection. There was low radioactivity (<0.8 %ID/g) accumulated in blood and normal organs except kidneys at all time points investigated. Introduction of a negatively-charged linker (-Gly-Glu-) into the peptide sequence decreased the renal uptake by 44% without affecting the tumor uptake at 4 h post-injection. High receptor-mediated melanoma uptakes coupled with fast whole-body clearance in B16/F1 melanoma-bearing C57 mice demonstrated the feasibility of using ^{111}In-labeled lactam bridge-cyclized α-MSH peptide analogues as a novel class of imaging probes for receptor-targeting melanoma imaging.

Keywords

Melanoma imaging; lactam bridge cyclization; alpha-MSH; melanocortin-1

Corresponding author: Yubin Miao, 2502 Marble NE, MSC09 5360, College of Pharmacy, University of New Mexico, Albuquerque, NM 87131-0001. Phone: (505) 925-4437; Fax: (505) 272-6749; ymiao@salud.unm.edu.

Introduction

Skin cancer is the most commonly diagnosed cancer in the United States. Malignant melanoma is the most lethal form of skin cancer and the most commonly diagnosed malignancy among young adults with an increasing incidence. It is predicted that there will be 59,940 cases of malignant melanoma newly reported and 8,110 fatalities in 2007 (1). There is a great need to develop novel imaging probes and treatment approaches for melanoma detection and therapy since early diagnosis and prompt surgical removal are a patient's best hope for a cure. Although 2-[^{18}F]fluoro-2-deoxy-D-glucose ([^{18}F]FDG) is commonly used for positron emission tomography (PET) diagnosis and staging of melanoma, [^{18}F]FDG is not melanoma-specific and some melanoma cells are not detected by [^{18}F]FDG since they use substrates other than glucose as energy sources (2, 3). Alternatively, the G protein-coupled melanocortin-1 (MC1) receptors have been used as targets for melanoma imaging peptides due to their over-expression on human and mouse melanoma cells (4-8). Radiolabeled α-melanocyte stimulating hormone (α-MSH) peptide analogues, derived from wild-type α-MSH, are very promising candidates for melanoma imaging and therapy due to their nanomolar MC1 receptor binding affinities and high receptor-mediated tumor uptakes in murine melanoma-bearing mice and human melanoma xenografts (9-13).

The strategy of peptide cyclization was used to improve binding affinity, *in vivo* stability and receptor selectivity of the α-MSH peptides (14-16). Compared to the linear peptides, the cyclic peptides possess less conformational freedom due to the stabilization of secondary structures such as beta turns, which results in greater receptor binding affinities. Furthermore, the constrained cyclic peptides confer higher stability against the proteolytic degradations *in vivo* (17). Peptide cyclization strategies can be generally classified into four types, namely, 1) backbone to backbone; 2) N-terminus to C-terminus; 3) one side chain to C-terminus or N-terminus; 4) two side chains via disulfide or lactam bridges. Over the past several years, peptide cyclization through metal coordination has been successfully employed in developing radiolabeled cyclic α-MSH peptide analogues for melanoma imaging and therapy. Metal cyclization made the α-MSH peptide analogues resistant to chemical and proteolytic degradation *in vivo* (18, 19). ^{111}In-DOTA-Re[Cys^{3,4,10}, D-Phe^{7}]-α-MSH$_{3\text{-}13}$} (^{111}In-DOTA-ReCCMSH) exhibited 11.4±2.89 %injected dose/gram (%ID/g) tumor uptake 2 h post-injection in B16/F1 murine melanoma mouse model (19). A comparison of biodistribution data between ^{111}In-labeled DOTA-conjugated metal-cyclized and disulfide bridge-cyclized α-MSH peptide analogues demonstrated that the metal cyclization resulted in more favorable pharmacokinetics of radiolabeled peptides, such as higher tumor uptake and lower renal uptake values (19), indicating that the different cyclization strategies might dramatically affect the biodistribution properties of peptides with comparable *in vitro* binding affinities.

In this study, Lys-Asp lactam bridge cyclization was employed to the α-MSH peptides to examine its effect on melanoma targeting and pharmacokinetics of the radiolabeled peptides. Two novel DOTA-conjugated lactam bridge-cyclized α-MSH peptide analogues, namely DOTA-CycMSH and DOTA-GlyGlu-CycMSH, were synthesized and characterized by liquid chromatography-mass spectrometry (LC-MS). A negatively-charged linker of -Gly-Glu- was introduced between DOTA and CycMSH sequences to determine its effect in reducing the renal uptake value of the radiolabeled peptide. The pharmacokinetics and SPECT/CT imaging of ^{111}In-labeled lactam bridge-cyclized α-MSH peptides were determined in B16/F1 melanoma-bearing C57 mice to evaluate their potential as SPECT imaging probes for melanoma detection.

Experimental Procedures

Chemicals and Reagents

Amino acid and resin were purchased from Advanced ChemTech Inc. (Louisville, KY) and Novabiochem (San Diego, CA). DOTA-tri-t-butyl ester was purchased from Macrocyclics Inc. (Richardson, TX). $^{111}InCl_3$ was purchased from Mallinckrodt, Inc. (St. Louis, MO). All other chemicals used in this study were purchased from Thermo Fischer Scientific (Waltham, MA) and used without further purification. B16/F1 murine melanoma cells were obtained from American Type Culture Collection (Manassas, VA).

Peptide Synthesis

Intermediate scaffold of H_2N-Lys(Dde)-Nle-Glu(OtBu)-His(Trt)-$_D$Phe-Arg(Pbf)-Trp(Boc)-Gly-Arg(Pbf)-Pro-Val was synthesized on Val-2-Chlorotrityl Chloride (Val-2ClTrt) resin using standard 9-fluorenylmethyloxycarbonyl (Fmoc) chemistry by an Advanced ChemTech multiple-peptide synthesizer (Louisville, KY). A small aliquot of the scaffold material was cleaved and characterized by LC-MS. Gly-Glu(OtBu) and DOTA-tri-t-butyl ester were manually attached to the intermediate scaffold using standard Fmoc chemistry, respectively. Protected branched peptide was cleaved from the resin treating with 25% hexafluoroisopropanol (HFIP) and 5% triisopropylsilane (TIS) in dichloromethane (DCM) and characterized by LC-MS. Peptide cyclization between the acid moiety of Val and the amino group of Asp coupled to the Lys side chain was achieved by overnight reaction in DMF in presence of 1 mM 1-hydroxybenzotriazole (HOBT), 2-(1H-benzotriazole-1-yl)-1,1,3,3-tetranethyluronium hexafluorophosphate (HBTU) and N,N-diisopropylethylamine (DIEA) mixture. The protecting groups were totally removed by treating with a mixture of trifluoroacetic acid (TFA), thioanisole, phenol, water, ethanedithiol and triisopropylsilane (87.5:2.5:2.5:2.5:2.5:2.5) for 2 h at room temperature (25°C). The peptides were precipitated and washed with ice-cold ether for four times. The final products were purified by RP-HPLC and characterized by LC-MS.

In vitro Competitive Binding Assay

The IC_{50} values of DOTA-CycMSH and DOTA-GlyGlu-CycMSH were determined by using methods described previously (8). B16/F1 cells were harvested and seeded into a 24-well cell culture plate (5×10^5/well) and incubated at 37°C overnight. After being washed once with binding media (MEM with 25 mM HEPES, pH 7.4, 0.2% BSA, 0.3 mM 1,10-phenathroline), the cells were incubated at room temperature (25°C) for 2 h with approximately 50,000 cpm of ^{125}I-Tyr^2-[Nle^4, $_D$-Phe^7]-α-MSH {NDP-MSH} (GE HealthCare, Piscataway, NJ) in presence of increasing concentrations of DOTA-CycMSH or DOTA-GlyGlu-CycMSH in 0.3 ml of binding media. The reaction media were aspirated after incubation. Cells were rinsed with 0.5 ml of ice-cold pH 7.4, 0.2% BSA / 0.01 M PBS twice and lysed in 0.5 ml of 1 N NaOH for 5 minutes. The activities in cells were measured in a gamma counter. The IC_{50} values for the peptides were calculated by using the Grafit software (Erithacus Software Limited, UK).

Complexation of the Peptide with ^{111}In

^{111}In-DOTA-CycMSH and ^{111}In-DOTA-GlyGlu-CycMSH were prepared using a 0.5 M NH_4OAc-buffered solution at pH 5.4. Briefly, 50 μl of $^{111}InCl_3$ (18.5-37.0 MBq in 0.05 M HCl), 10 μl of 1 mg/ml DOTA-CycMSH or DOTA-GlyGlu-CycMSH aqueous solution and 400 μl of 0.5 M NH_4OAc (pH 5.4) were added into a reaction vial and incubated at 75°C for 45 min. After the incubation, 20 μl of 0.5% EDTA aqueous solution was added into the reaction vial to scavenge potential unbound ^{111}In. The radiolabeled complexes were purified to single species by Waters RP-HPLC (Milford, MA) on a Grace Vadyc C-18 reverse phase

analytical column (Deerfield, IL) using a 20-minute gradient of 16-26% acetonitrile in 20 mM HCl aqueous solution with a flowrate of 1 ml/min. Purified peptide samples were purged with N_2 gas for 20 minutes to remove the acetonitrile. The pH of final solution was adjusted to 7.4 with 0.1 N NaOH and normal saline for animal studies. The stability of ^{111}In-DOTA-CycMSH and ^{111}In-DOTA-GlyGlu-CycMSH was determined by incubation in mouse serum at 37°C according to the published procedure (20) for various time periods, and monitored for degradation by RP-HPLC.

Cellular Internalization and Efflux of ^{111}In-labeled Peptides

Cellular internalization and efflux of ^{111}In-DOTA-CycMSH and ^{111}In-DOTA-GlyGlu-CycMSH were evaluated in B16/F1 cells as described by Miao *et al* (21). After being washed once with binding media (MEM with 25 mM HEPES, pH 7.4, 0.2% BSA, 0.3 mM 1,10-phenathroline), B16/F1 cells in cell culture plates were incubated at 25°C for 20, 40, 60, 90 and 120 min (n=4) in presence of approximately 200,000 counts per minute (cpm) of HPLC purified ^{111}In-DOTA-CycMSH (0.019 pmol) or ^{111}In-DOTA-GlyGlu-CycMSH (0.019 pmol). After incubation, the reaction media were aspirated and cells were rinsed with 2×0.5 ml of ice-cold pH 7.4, 0.2% BSA / 0.01 M PBS. Cellular internalization of radiolabeled peptides was assessed by washing the cells with acidic buffer [40 mM sodium acetate (pH 4.5) containing 0.9% NaCl and 0.2% BSA] to remove the membrane-bound radioactivity. The remaining internalized radioactivity was obtained by lysing the cells with 0.5 ml of 1N NaOH for 5 min. Membrane-bound and internalized ^{111}In activities were counted in a gamma counter. Cellular efflux of radiolabeled peptides was determined by incubating B16/F1 cells with ^{111}In-DOTA-CycMSH and ^{111}In-DOTA-GlyGlu-CycMSH for 2 h at 25°C, removing non-specific-bound activity with 2×0.5 ml of ice-cold pH 7.4, 0.2% BSA / 0.01 M PBS rinse, and monitoring radioactivity released into cell culture media. At time points of 20, 40, 60, 90 and 120 min, the radioactivities in media, on cell surface and in cells were separately collected and counted in a gamma counter.

Biodistribution Studies

All the animal studies were conducted in compliance with Institutional Animal Care and Use Committee approval. The pharmacokinetics of ^{111}In-DOTA-CycMSH and ^{111}In-DOTA-GlyGlu-CycMSH were determined in B16/F1 murine melanoma-bearing C57 female mice (Harlan, Indianapolis, IN). C57 mice were inoculated subcutaneously with 1×10^6 B16/F1 murine melanoma cells in the right flank. After 10 days, when the weight of tumors reached approximately 0.2 g, 0.037 MBq of ^{111}In-DOTA-CycMSH or ^{111}In-DOTA-GlyGlu-CycMSH was injected into each mouse through the tail vein. Groups of 5 mice were sacrificed at 2, 4 and 24 h post-injection, and tumors and organs of interest were harvested, weighed and counted. Blood values were taken as 6.5% of the whole-body weight. The tumor uptake specificity of ^{111}In-DOTA-CycMSH and ^{111}In-DOTA-GlyGlu-CycMSH was determined by blocking tumor uptake with the co-injection of 10 μg (6.07 nmol) of unlabeled NDP-MSH, a linear α-MSH peptide analogue with picomolar affinity for the MC1 receptors present on murine melanoma cells. Statistical analysis was performed using the Student's t-test for unpaired data. A 95% confidence level was chosen to determine the significance between radiolabeled compounds, with $p<0.05$ being significantly different.

Imaging Melanoma with ^{111}In-DOTA-CycMSH and ^{111}In-DOTA-GlyGlu-CycMSH

Two B16/F1 melanoma-bearing C57 mice were injected with 13.7 MBq of ^{111}In-DOTA-CycMSH or ^{111}In-DOTA-GlyGlu-CycMSH via the tail vein, respectively. The mice were euthanized for micro-CT imaging immediately followed by micro-SPECT imaging at 2 h post-injection. Micro-SPECT scans of 60 frames for each animal were acquired and total counts acquisitions of 524,672 and 278,242 counts (2 h acquisition) were achieved for both SPECT scans, respectively. The micro-SPECT images were obtained using the Micro-CAT

II CT/SPECT (Siemens) unit equipped with high resolution 2 mm pinhole collimators (22). Reconstructed data from SPECT and CT were visualized and co-registered using Amira 3.1 (Ascent Media System & Technology Service, Northvale, NJ).

Urinary Metabolites of ^{111}In-DOTA-CycMSH and ^{111}In-DOTA-GlyGlu-CycMSH

One hundred microliter of HPLC purified ^{111}In-DOTA-CycMSH (0.74-1.11 MBq, 0.82-1.12 ng) or ^{111}In-DOTA-GlyGlu-CycMSH (0.74-1.11 MBq, 0.90-1.35 ng) was injected into each B16/F1 murine melanoma-bearing C57 mouse through the tail vein. At 2 h after dose administration, mice were sacrificed and the urine was collected. The radioactive metabolites in the urine were analyzed by injecting aliquots of urine into HPLC. A 20-minute gradient of 16-26% acetonitrile / 20 mM HCl was used for the urine analysis.

Results

DOTA-CycMSH and DOTA-GlyGlu-CycMSH were synthesized, purified by RP-HPLC and the identities of peptides were confirmed by electrospray ionization mass spectrometry. The synthetic schemes are presented in Fig. 1. The competitive binding curves of DOTA-CycMSH and DOTA-GlyGlu-CycMSH are shown in Fig. 2. The IC_{50} values of DOTA-CycMSH and DOTA-GlyGlu-CycMSH were 1.75 nM and 0.90 nM in B16/F1 cells. The peptides were labeled with ^{111}In using a 0.5 M NH_4OAc-buffered solution at pH 5.4. The radiolabeling yields were greater than 95% for both peptides. ^{111}In-DOTA-CycMSH and ^{111}In-DOTA-GlyGlu-CycMSH were completely separated from their excess non-labeled peptides by RP-HPLC. The retention times of ^{111}In-DOTA-CycMSH and ^{111}In-DOTA-GlyGlu-CycMSH were 15.4 and 18.0 min, respectively. The specific activities of ^{111}In-DOTA-CycMSH and ^{111}In-DOTA-GlyGlu-CycMSH were 9.03×10^8 and 8.23×10^8 MBq/g, respectively. ^{111}In-DOTA-CycMSH and ^{111}In-DOTA-GlyGlu-CycMSH were stable in mouse serum at 37°C. Only the ^{111}In-labeled peptides were detected by RP-HPLC after 24 h of incubation (Fig. 3).

Cellular internalization and efflux of ^{111}In-DOTA-CycMSH and ^{111}In-DOTA-GlyGlu-CycMSH were evaluated in B16/F1 cells at 25°C. Figure 4 illustrates cellular internalization and efflux of ^{111}In-DOTA-CycMSH and ^{111}In-DOTA-GlyGlu-CycMSH. Both ^{111}In-DOTA-CycMSH and ^{111}In-DOTA-GlyGlu-CycMSH exhibited rapid cellular internalization and extended cellular retention. There were 73.71±1.71% of the ^{111}In-DOTA-CycMSH and 66.19±2.12% of the ^{111}In-DOTA-GlyGlu-CycMSH activity internalized in the B16/F1 cells 40 min post incubation. There were 81.98±2.02% of the ^{111}In-DOTA-CycMSH and 78.93±0.64% of the ^{111}In-DOTA-GlyGlu-CycMSH activity internalized in the cells after 2 h incubation. Cellular efflux experiments demonstrated that 90.26±1.71% of the ^{111}In-DOTA-CycMSH activity and 90.00±1.10% of the ^{111}In-DOTA-GlyGlu-CycMSH activity remained inside the cells 2 h after incubating cells in culture media at 25°C.

The pharmacokinetics and tumor targeting properties of ^{111}In-DOTA-CycMSH and ^{111}In-DOTA-GlyGlu-CycMSH were determined in B16/F1 murine melanoma-bearing C57 mice. The biodistribution of ^{111}In-DOTA-CycMSH and ^{111}In-DOTA-GlyGlu-CycMSH are shown in Table 1. Both ^{111}In-DOTA-CycMSH and ^{111}In-DOTA-GlyGlu-CycMSH exhibited very rapid and high tumor uptakes. At 2 h post-injection, ^{111}In-DOTA-CycMSH and ^{111}In-DOTA-GlyGlu-CycMSH reached their peak tumor uptake values of 9.53±1.41 and 10.40±1.40 %ID/g, respectively. There were 7.54±0.70 %ID/g of the ^{111}In-DOTA-CycMSH and 7.40±0.43 %ID/g of the ^{111}In-DOTA-GlyGlu-CycMSH activities remained in the tumors 4 h post-injection. The tumor uptake values of ^{111}In-DOTA-CycMSH and ^{111}In-DOTA-GlyGlu-CycMSH decreased to 2.22±0.51 and 2.37±0.28 %ID/g at 24 h post-injection. In competition studies, the tumor uptakes of ^{111}In-DOTA-CycMSH and ^{111}In-DOTA-GlyGlu-CycMSH with 10 μg (6.07 nmol) of non-radiolabeled NDP co-injection

were only 3.0% and 2.6% of the tumor uptake without NDP co-injection at 2 h after dose administration ($P<0.01$), demonstrating that the tumor uptakes were specific and receptor-mediated. Whole-body clearance of ^{111}In-DOTA-CycMSH and ^{111}In-DOTA-GlyGlu-CycMSH was very rapid, with approximately 90% of the injected radioactivity cleared through the urinary system by 2 h post-injection (Table 1). Normal organ uptakes of ^{111}In-DOTA-CycMSH and ^{111}In-DOTA-GlyGlu-CycMSH were generally very low (<0.8 %ID/g) except for the kidneys at all time points investigated in this study. High tumor/blood and tumor/normal organ uptake ratios were demonstrated 2 h post-injection (Table 1). Although there was no statistical difference in tumor uptake between ^{111}In-DOTA-CycMSH and ^{111}In-DOTA-GlyGlu-CycMSH, the renal uptake of ^{111}In-DOTA-GlyGlu-CycMSH was significantly lower ($p<0.05$, Table 1) than that of ^{111}In-DOTA-CycMSH at 2, 4 and 24 h post-injection. ^{111}In-DOTA-GlyGlu-CycMSH displayed 44% less renal uptake value than ^{111}In-DOTA-CycMSH at 4 h post-injection. At 24 h after dose administration, the kidney uptake values of ^{111}In-DOTA-CycMSH and ^{111}In-DOTA-GlyGlu-CycMSH decreased to 16.00±2.30 and 9.06±1.82 %ID/g, respectively. Bone uptake values of ^{111}In-DOTA-CycMSH and ^{111}In-DOTA-GlyGlu-CycMSH were low (<0.2 %ID/g) at all time points investigated in this study.

Two B16/F1 murine melanoma-bearing C57 mice were separately injected with ^{111}In-DOTA-CycMSH (13.7 MBq, 15.2 ng) and ^{111}In-DOTA-GlyGlu-CycMSH (13.7 MBq, 16.6 ng) through the tail vein to visualize the tumors at 2 h after dose administration. The whole-body SPECT images of the mice were fused with CT images, respectively. The transaxial tumor images and the whole-body images are presented in Fig. 5. Flank melanoma tumors were visualized clearly by both ^{111}In-DOTA-CycMSH and ^{111}In-DOTA-GlyGlu-CycMSH at 2 h post-injection. Both ^{111}In-DOTA-CycMSH and ^{111}In-DOTA-GlyGlu-CycMSH exhibited high tumor to normal organ uptake ratios except for the kidney, which was coincident with the trend observed in the biodistribution results. In view of the substantial renal uptake values of ^{111}In-DOTA-CycMSH and ^{111}In-DOTA-GlyGlu-CycMSH in the biodistribution results, the urinary metabolites of ^{111}In-DOTA-CycMSH and ^{111}In-DOTA-GlyGlu-CycMSH were analyzed by RP-HPLC at 2 h post-injection. The HPLC elution profiles of ^{111}In-DOTA-CycMSH and ^{111}In-DOTA-GlyGlu-CycMSH are shown in Fig. 6. All of ^{111}In-DOTA-CycMSH and ^{111}In-DOTA-GlyGlu-CycMSH were transformed to two more polar metabolites at 2 h post-injection, respectively.

Discussion

Previous publications have demonstrated that the cyclization of α-MSH peptide analogues was able to improve the binding affinities and *in vivo* stability of peptides (14-16). The cyclic peptides possess less conformational freedom and higher stability than the linear peptides due to the stabilization of secondary structures, such as beta turns. The stabilization of secondary structures makes the cyclic peptides better fit receptor binding pocket, enhancing the binding affinities of the cyclic peptides. Peptide cyclization can be achieved through disulfide bridges, lactam bridges, covalent bonds such as N-N and N-C bonds or metal coordination. Site-specific bond formation or metal coordination allows one to control the ring size of the cyclic peptide, which is critical for optimal receptor binding. Over the past several years, we have successfully employed radiometal to cyclize CCMSH peptides through radiolabeling processes (6, 7, 18). Labeling the CCMSH peptides with ^{99m}Tc or ^{188}Re simultaneously completed the peptide cyclization and the coupling of radionuclides to the peptides for melanoma imaging or therapy. The metal cyclization made α-MSH peptide analogues resistant to chemical and proteolytic degradation *in vivo* (18, 19). Furthermore, the metal cyclization resulted in greater tumor uptake and lower renal uptake values of the radiolabeled peptides compared to the disulfide bridge cyclization (19),

demonstrating that the different cyclization strategies affect the biodistribution properties of radiolabeled peptides with similar *in vitro* receptor binding affinities.

Two novel lactam bridge-cyclized α-MSH peptide analogues were synthesized to examine the effect of lactam bridge cyclization on the tumor targeting and pharmacokinetics of the radiolabeled peptides. DOTA-CycMSH and DOTA-GlyGlu-CycMSH displayed IC_{50} values of 1.75 and 0.9 nM, that were comparable to metal- and disulfide-cyclized α-MSH peptide analogues previously reported (19). The lactacm bridge cyclization remained the nanomolar receptor binding affinities of the peptides, demonstrating its suitability and feasibility as a strategy to cyclize the peptides. Both ^{111}In-DOTA-CycMSH and ^{111}In-DOTA-GlyGlu-CycMSH exhibited rapid cellular internalization and extended cellular retention in B16/F1 cells, with approximately 70% of the activity internalized in the cells 40 min post incubation and 90% of internalized activity remained in the cells after 2 h incubation in culture media. Efficient cellular internalization coupled with extended retention made the lactam bridge-cyclized α-MSH peptide analogues suitable for melanoma imaging and therapy (6, 23).

Both ^{111}In-DOTA-CycMSH and ^{111}In-DOTA-GlyGlu-CycMSH exhibited high receptor-mediated tumor uptakes of 9.53±1.41 and 10.40±1.40 %ID/g at 2 h post-injection, respectively. The tumor uptakes of ^{111}In-DOTA-CycMSH and ^{111}In-DOTA-GlyGlu-CycMSH (lactam bridge-cyclized α-MSH peptides) were comparable to that of ^{111}In-DOTA-ReCCMSH (a metal-cyclized α-MSH peptide), but slightly higher than the tumor uptake of ^{111}In-DOTA-[Cys^{4,10}, D-Phe^{7}]-α-MSH$_{4-13}$ (^{111}In-DOTA-CMSH, a disulfide bridge-cyclized α-MSH peptide) (19). Two novel ^{111}In-labeled DOTA-conjugated linear α-MSH peptide analogues, [Nle^{4}, Asp^{5}, D-Phe^{7}, Lys^{11}(DOTA)-^{111}In]-α-MSH$_{4-11}$ (^{111}In-DOTA-NAPamide) and ^{111}In-DOTA-[β-Ala^{3}, Nle^{4}, Asp^{5}, D-Phe^{7}, Lys^{10}]-α-MSH$_{3-10}$ (^{111}In-DOTA-MSH$_{oct}$), were reported for melanoma imaging (11, 12). ^{111}In-DOTA-NAPamide displayed greater tumor uptake values and better pharmacokinetics than ^{111}In-DOTA-MSH$_{oct.}$ The tumor uptake values of ^{111}In-DOTA-NAPamide were 7.56±0.51 %ID/g at 4 h and 2.32±0.28 %ID/g at 24 h post-injection in the B16/F1 melanoma mouse model (12). Both ^{111}In-DOTA-CycMSH and ^{111}In-DOTA-GlyGlu-CycMSH exhibited comparable tumor uptake values with ^{111}In-DOTA-NAPamide at 4 and 24 h post-injection. Flank melanoma tumors were clearly visualized with ^{111}In-DOTA-CycMSH and ^{111}In-DOTA-GlyGlu-CycMSH at 2 h post-injection by SPECT/CT images (Fig. 5). The SPECT imaging of tumors accurately matched the anatomical information from CT images. ^{111}In-DOTA-CycMSH and ^{111}In-DOTA-GlyGlu-CycMSH displayed high tumor to normal organ uptake ratios except for the kidney, which was coincident with the trend observed in biodistribution results. The high receptor-mediated tumor uptake and tumor to normal organ uptake ratios highlighted the potential of radiolabeled lactam bridge-cyclized α-MSH peptides as a novel class of peptide radiopharmaceuticals for melanoma imaging.

Both biodistribution results and SPECT/CT images demonstrated that the kidney was primary excretion pathway of the radiolabeled lactam bridge-cyclized α-MSH peptides. The strategy of infusing basic amino acids such as lysine or arginine has been employed to decrease the renal uptakes of radiolabeled peptides by shielding the electrostatic interaction between positively-charged peptides and negatively-charged surface of tubule cells (7, 24, 25). Recently, it has been reported that different pathways may play roles in the mechanism of the renal uptake of radiolabeled peptides besides the electrostatic interaction between the positively-charged peptides and negatively-charged tubule cells (26, 27). For instance, the use of colchicine, which prevents endocytosis in tubular cells, has successfully decreased the renal uptake up to 25% in a rat model (27). Moreover, transmembrane glycoproteins such as megalin, have been reported to be involved in the renal uptakes of radiolabeled somatostatin analogues (28). Since the extracellular domains of megalin can accommodate a variety of ligands, megalin may be involved in the renal uptakes of other radiolabeled peptides.

Glutamic acid has been introduced into the peptide sequences to reduce the renal uptakes of radiolabeled metal-cyclized α-MSH peptides (29), as well as a PKM linker to modify the biodistribution of radiolabeld RGD peptides (30-35). In this study, the structural modification of increasing the overall negative charge of the peptide (introducing a glutamic acid) was investigated to demonstrate whether the structural modification could reduce the renal uptake values of the radiolabeled peptides. As a matter of fact, the introduction of a negatively-charged glutamic acid as a linker significantly ($p<0.05$) decreased the renal uptake of ^{111}In-DOTA-GlyGlu-CycMSH by 44% compared to ^{111}In-DOTA-CycMSH (Table 1) 4 h post-injection, suggesting that the electrostatic interaction played an important role in the renal uptakes of ^{111}In-DOTA-CycMSH and ^{111}In-DOTA-GlyGlu-CycMSH. The urine analysis showed that both ^{111}In-DOTA-CycMSH and ^{111}In-DOTA-GlyGlu-CycMSH were metabolized into two moieties that might be responsible for the activity retention in kidneys. The kidney uptake value of ^{111}In-DOTA-GlyGlu-CycMSH was 29% higher than ^{111}In-DOTA-ReCCMSH at 4 h post-injection. However, the renal uptake value of ^{111}In-DOTA-GlyGlu-CycMSH was only 34% of that of ^{111}In-DOTA-CMSH at 4 h post-injection, demonstrating that the lactam cyclization was better than the disulfide cyclization in terms of less renal uptake value. Introduction of one more negatively-charged glutamic acid or lysine co-injection might further decrease the renal uptake of ^{111}In-DOTA-GlyGlu-CycMSH. Another potential strategy to further reduce the kidney uptake would be to use shorter lactam bridge-cyclized α-MSH peptide since lower molecular weight ^{111}In-DOTA-NAPamide exhibited less kidney uptake than ^{111}In-DOTA-GlyGlu-CycMSH. Further reduction of the renal uptakes will facilitate the clinical evaluations of this novel class of radiolabeled α-MSH peptides as melanoma imaging probes, as well as promote the potential use of this novel class of radiolabeled α-MSH peptides as therapeutic agents for peptide-targeted radionuclide therapy of melanoma.

In conclusion, ^{111}In-labeled DOTA-conjugated lactam bridge-cyclized α-MSH peptides exhibited high receptor-mediated tumor uptake coupled with fast whole-body clearance in B16/F1 murine melanoma model. Introduction of a negatively-charged linker (-Gly-Glu-) into the peptide sequence decreased the renal uptakes by 44% without affecting the tumor uptakes 4 h post-injection. ^{111}In-labeled lactam bridge-cyclized α-MSH peptide analogues appear to be a novel class of very promising peptide radiopharmaceuticals for receptor-targeting melanoma imaging.

Acknowledgments

The authors express their gratitude to Drs. Wynn A. Volkert and Susan L. Deutscher for their helpful discussions. The authors thank Drs. Said D. Figueroa, Timothy J. Hoffman and Ms. Tiffani Shelton, Katherine Benwell for their assistance.

Grant support: UNM-LANL MOU on Research and Education Grant 2R76T (Y.M), American Foundation for Pharmaceutical Education Grant 3R48E (Y.M) and American Cancer Society Institutional Research Grant IRG-92-024 (Y.M) and National Cancer Institute P50 Imaging Center Grant P50-CA-103130 (T.P.Q)

References

1. Jemal A, Siegel R, Ward E, Murray T, Xu J, Thun MJ. Cancer statistics, 2007. CA Cancer J Clin. 2007; 57:43–66. [PubMed: 17237035]
2. Nabi HA, Zubeldia JM. Clinical application of 18F-FDG in oncology. J Nucl Med Technol. 2002; 30:3–9. [PubMed: 11948260]
3. Dimitrakopoulou-Strauss A, Strauss LG, Burger C. Quantitative PET studies in pretreated melanoma patients: A comparison of 6-[^{18}F]fluoro-L-DOPA with ^{18}F-FDG and ^{15}O-water using compartment and non-compartment analysis. J Nucl Med. 2001; 42:248–256. [PubMed: 11216523]

4. Tatro JB, Reichlin S. Specific receptors for alpha-melanocyte-stimulating hormone are widely distributed in tissues of rodents. Endocrinology. 1987; 121:1900–1907. [PubMed: 2822378]
5. Siegrist W, Solca F, Stutz S, Giuffre L, Carrel S, Girard J, Eberle AN. Characterization of receptors for alpha-melanocyte-stimulating hormone on human melanoma cells. Cancer Res. 1989; 49:6352–6358. [PubMed: 2804981]
6. Chen J, Cheng Z, Hoffman TJ, Jurisson SS, Quinn TP. Melanoma-targeting properties of ^{99m}Technetium-labeled cyclic α-melanocyte-stimulating hormone peptide analogues. Cancer Res. 2000; 60:5649–5658. [PubMed: 11059756]
7. Miao Y, Owen NK, Whitener D, Gallazzi F, Hoffman TJ, Quinn TP. In vivo evaluation of ^{188}Re-labeled alpha-melanocyte stimulating hormone peptide analogs for melanoma therapy. Int J Cancer. 2002; 101:480–487. [PubMed: 12216078]
8. Miao Y, Whitener D, Feng W, Owen NK, Chen J, Quinn TP. Evaluation of the human melanoma targeting properties of radiolabeled alpha-Melanocyte stimulating hormone peptide analogues. Bioconjug Chem. 2003; 14:1177–1184. [PubMed: 14624632]
9. Miao Y, Owen NK, Fisher DR, Hoffman TJ, Quinn TP. Therapeutic efficacy of a ^{188}Re labeled α-melanocyte stimulating hormone peptide analogue in murine and human melanoma-bearing mouse models. J Nucl Med. 2005; 46:121–129. [PubMed: 15632042]
10. Miao Y, Hylarides M, Fisher DR, Shelton T, Moore H, Wester DW, Fritzberg AR, Winkelmann CT, Hoffman TJ, Quinn TP. Melanoma therapy via peptide-targeted α-radiation. Clin Cancer Res. 2005; 11:5616–5621. [PubMed: 16061880]
11. Froidevaux S, Calame-Christe M, Tanner H, Sumanovski L, Eberle AN. A novel DOTA-α-melanocyte-stimulating hormone analog for metastatic melanoma diagnosis. J Nucl Med. 2002; 43:1699–1706. [PubMed: 12468522]
12. Froidevaux S, Calame-Christe M, Schuhmacher J, Tanner H, Saffrich R, Henze M, Eberle AN. A Gallium-labeled DOTA-α-melanocyte-stimulating hormone analog for PET imaging of melanoma metastases. J Nucl Med. 2004; 45:116–123. [PubMed: 14734683]
13. Froidevaux S, Calame-Christe M, Tanner H, Eberle AN. Melanoma targeting with DOTA-alpha-melanocyte-stimulating hormone analogs: structural parameters affecting tumor uptake and kidney uptake. J Nucl Med. 2005; 46:887–895. [PubMed: 15872364]
14. Sawyer TK, Hruby VJ, Darman PS, Hadley ME. [half-Cys^{4},half-Cys^{10}]-α-melanocyte-stimulating hormone: a cyclic α-melanotropin exhibiting superagonist biological activity. Proc Natl Acad Sci U S A. 1982; 79:1751–1755. [PubMed: 6281785]
15. Al-Obeidi F, Hadley ME, Pettitt BM, Hruby VJ. Design of a new class of superpotent cyclic a-melanotropins based on quenched dynamic simulations. J Am Chem Soc. 1989; 111:3413–3416.
16. Al-Obeidi F, de L Castrucci AM, Hadley ME, Hruby VJ. Potent and prolonged-acting cyclic lactam analogs of a-melanotropin: design based on molecular dynamics. J Med Chem. 1989; 32:2555–2561. [PubMed: 2555512]
17. Fung S, Hruby VJ. Design of cyclic and other templates for potent and selective peptide α-MSH analogues. Current Opinion in Chem Biol. 2005; 9:352–358.
18. Giblin MF, Wang NN, Hoffman TJ, Jurisson SS, Quinn TP. Design and charaterization of α-melanotropin peptide analogs cyclized through rhenium and technetium metal coordination. Proc Natl Acad Sci U S A. 1998; 95:12814–12818. [PubMed: 9788997]
19. Chen J, Cheng Z, Owen NK, Hoffman TJ, Miao Y, Jurisson SS, Quinn TP. Evaluation of an ^{111}In-DOTA-rhenium cyclized α-MSH analog: a novel cyclic-peptide analog with improved tumor-targeting properties. J Nucl Med. 2001; 42:1847–1855. [PubMed: 11752084]
20. Aloj L, Panico M, Caraco C, Del Vecchio S, Arra C, Affuso A, Accardo A, Mansi R, Tesauro D, De Luca S, Pedone C, Visentin R, Mazzi U, Morelli G, Salvatore M. *In vitro* and *in vivo* characterization of Indium-111 and Technetium-99m labeled CCK-8 derivatives for CCK-B receptor imaging. Cancer Biotherapy Radiopharm. 2004; 19:93–98.
21. Miao Y, Hoffman TJ, Quinn TP. Tumor-targeting properties of ^{90}Y- and ^{177}Lu-labeled α-melanocyte stimulating hormone peptide analogues in a murine melanoma model. Nucl Med Biol. 2005; 32:485–493. [PubMed: 15982579]

22. Miao Y, Benwell K, Quinn TP. ^{99m}Tc and ^{111}In labeled alpha-melanocyte stimulating hormone peptides as imaging probes for primary and pulmonary metastatic melanoma detection. J Nucl Med. 2007; 48:73–80. [PubMed: 17204701]
23. Volkert WA, Hoffman TJ. Therapeutic radiopharmaceuticals. Chem Rev. 1999; 99:2269–2292. [PubMed: 11749482]
24. Behr TM, Sharkey RM, Juweid ME, Blumenthal RD, Dunn RM, Bair HJ, Wolf FG, Becker WS, Goldenberg DM. Reduction of the renal uptake of radiolabeled monoclonal antibody fragments by cationic amino acids and their derivatives. Cancer Res. 1995; 55:3825–3834. [PubMed: 7641200]
25. Behr TM, Becker WS, Sharkey RM, Juweid ME, Dunn RM, Bair HJ, Wolf FG, Goldenberg DM. Reduction of renal uptake of monoclonal antibody fragments by amino acid infusion. J Nucl Med. 1996; 37:829–833. [PubMed: 8965154]
26. Béhé M, Kluge G, Becker W, Gotthardt M, Behr TM. Use of polyglutamic acids to reduce uptake of radiometal-labeled minigastrin in the kidneys. J Nucl Med. 2005; 46:1012–1015. [PubMed: 15937313]
27. Rolleman EJ, Krenning EP, Van Gameren A, Bernard BF, De Jong M. Uptake of [^{111}In-DTPA0]octreotide in the rat kidney is inhibited by colchicine and not by fructose. J Nucl Med. 2004; 45:709–713. [PubMed: 15073269]
28. De Jong M, Barone R, Krenning EP, Bernard BF, Melis M, Vissor T, Gekle M, Willnow TE, Walrand S, Jamar F, Pauwels S. Megalin is essential for renal proximal tubule reabsorption of ^{111}In-DTPA-Octreotide. J Nucl Med. 2005; 46:1696–1700. [PubMed: 16204720]
29. Miao Y, Fisher DR, Quinn TP. Reducing renal uptake of ^{90}Y and ^{177}Lu labeled alpha-melanocyte stimulating hormone peptide analogues. Nucl Med Biol. 2006; 33:723–733. [PubMed: 16934691]
30. Liu S, He Z, Hsieh WY, Kim YS, Jiang Y. Impact of PKM linkers on biodistribution characteristics of the ^{99m}Tc-labeled cyclic RGDfK dimer. Bioconjug Chem. 2006; 17:1499–1507. [PubMed: 17105229]
31. Dijkgraaf I, Liu S, Kruijtzer JA, Soede AC, Oyen WJ, Liskamp RM, Corstens FH, Boerman OC. Effects of linker variation on the in vitro and in vivo characteristics of an ^{111}In-labeled RGD peptide. Nucl Med Biol. 2007; 34:29–35. [PubMed: 17210459]
32. Liu S, Hsieh WY, Jiang Y, Kim YS, Sreerama SG, Chen X, Jia B, Wang F. Evaluation of a ^{99m}Tc-labeled cyclic RGD tetramer for noninvasive imaging integrin $\alpha_v\beta_3$-positive breast cancer. Bioconjug Chem. 2007; 18:438–446. [PubMed: 17341108]
33. Wu Y, Zhang X, Xiong Z, Cheng Z, Fisher DR, Liu S, Gambhir SS, Chen X. MicroPET imaging of glioma integrin $\alpha_v\beta_3$ expression using ^{64}Cu-labeled tetrameric RGD peptide. J Nucl Med. 2005; 46:1707–1718. [PubMed: 16204722]
34. Li ZB, Cai W, Cao Q, Chen K, Wu Z, He L, Chen X. ^{64}Cu-labeled tetrameric and octameric RGD peptides for small-animal PET of tumor $\alpha_v\beta_3$ integrin expression. J Nucl Med. 2007; 48:1162–1171. [PubMed: 17574975]
35. Dijkgraaf I, Kruijtzer JA, Liu S, Soede AC, Oyen WJ, Corstens FH, Liskamp RM, Boerman OC. Improved targeting of the alpha(v)beta(3) integrin by multimerisation of RGD peptides. Eur J Nucl Med Mol Imaging. 2007; 34:267–273. [PubMed: 16909226]

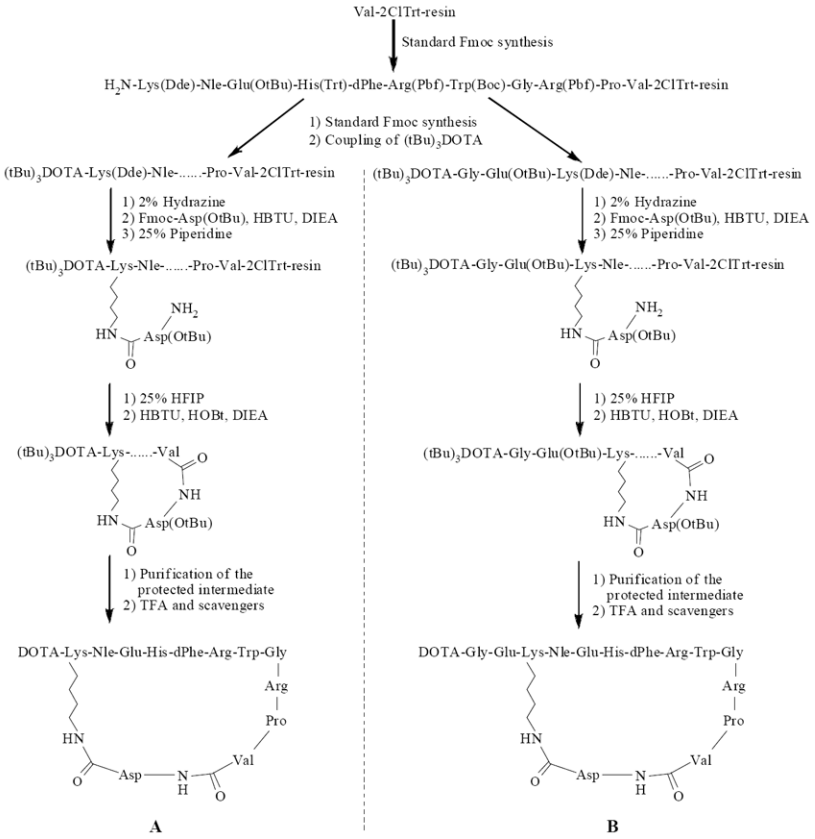

Figure 1.
Synthetic schemes of DOTA-CycMSH (A) and DOTA-GlyGlu-CycMSH (B).

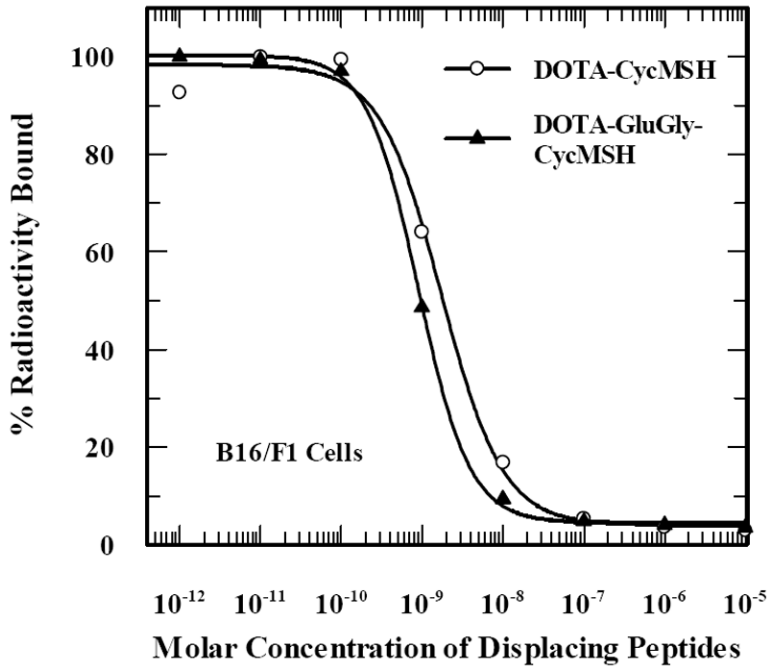

Figure 2.

The competitive binding curves of DOTA-CycMSH and DOTA-GlyGlu-CycMSH in B16/F1 murine melanoma cells. The IC_{50} values of DOTA-CycMSH and DOTA-GlyGlu-CycMSH were 1.75 nM and 0.90 nM.

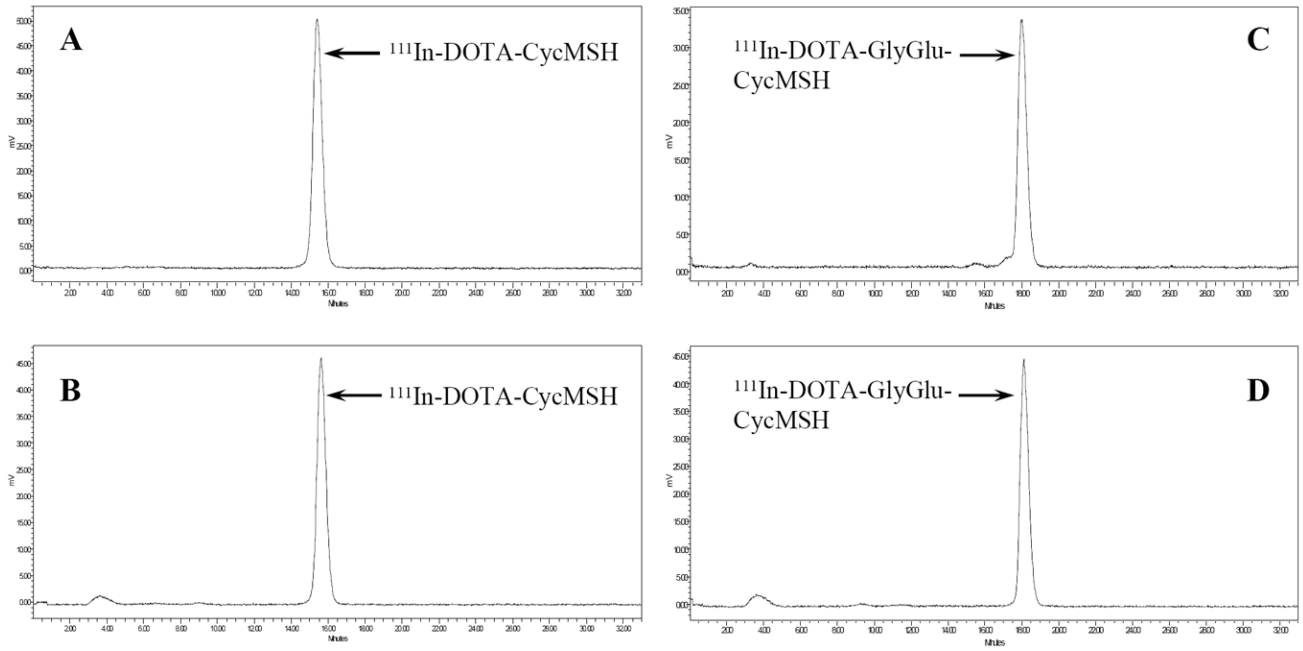

Figure 3.

HPLC profiles of radioactive ^{111}In-DOTA-CycMSH (A), ^{111}In-DOTA-GlyGlu-CycMSH (C) and mouse serum stability of ^{111}In-DOTA-CycMSH (B), ^{111}In-DOTA-GlyGlu-CycMSH (D) after 24 h incubation at 37°C, respectively. The retention times of ^{111}In-DOTA-CycMSH and ^{111}In-DOTA-GlyGlu-CycMSH were 15.4 and 18.0 min, respectively.

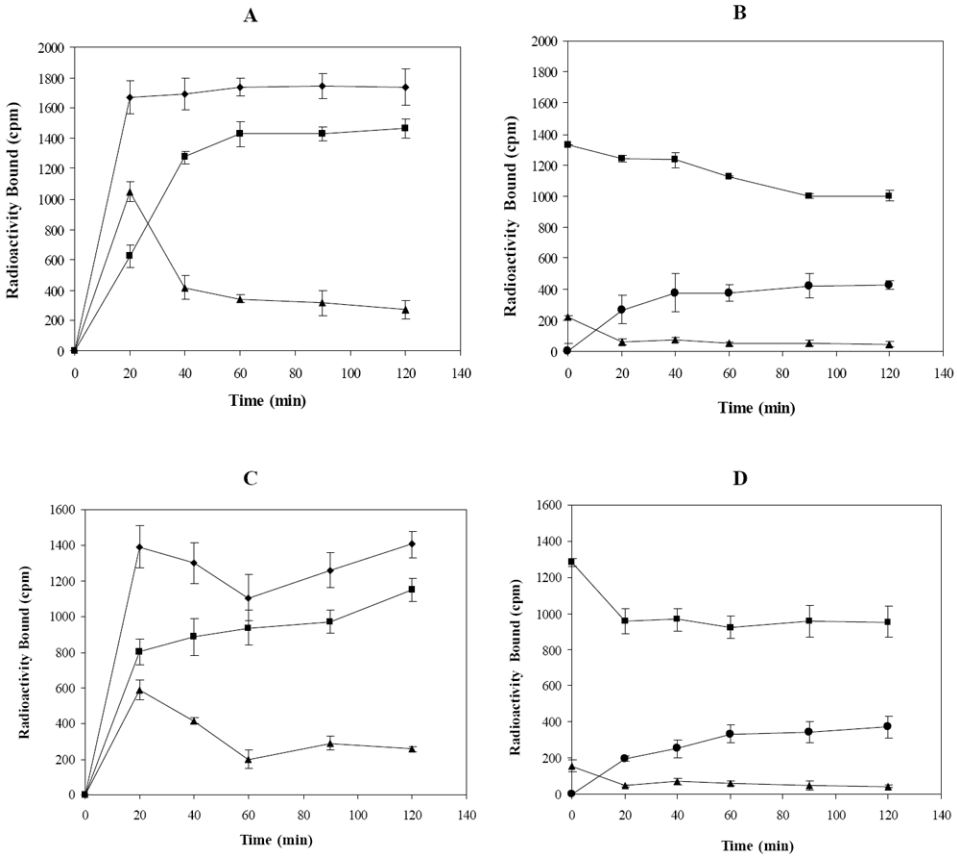

Figure 4.

Cellular internalization and efflux of ^{111}In-DOTA-CycMSH (A and B) and ^{111}In-DOTA-GlyGlu-CycMSH (C and D) in B16/F1 murine melanoma cells at 25°C. Total bound radioactivity (◆), internalized activity (■), cell membrane activity (▲) and cell culture media activity (●) were presented as counts per minute (cpm).

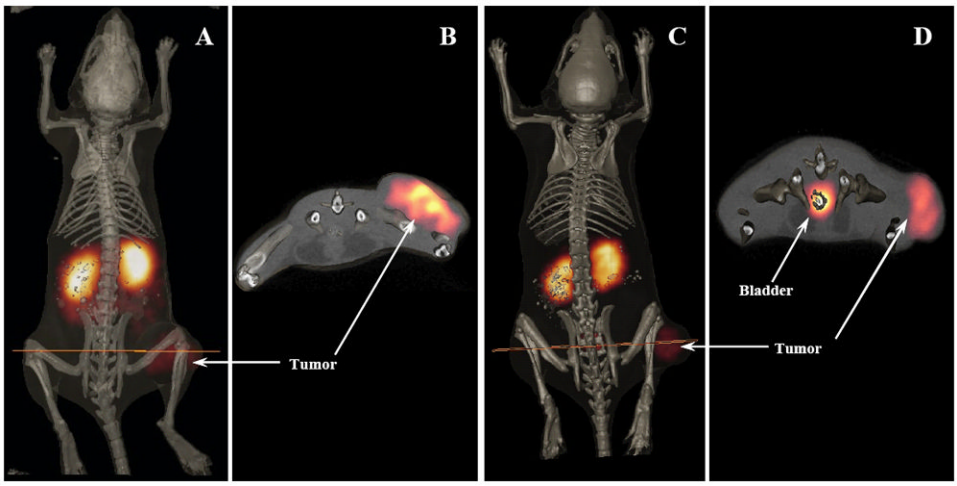

Figure 5.
Whole-body and transaxial images of ^{111}In-DOTA-CycMSH (A, B) and ^{111}In-DOTA-GlyGlu-CycMSH (C, D) in B16/F1 flank melanoma-bearing C57 mice at 2 h post-injection.

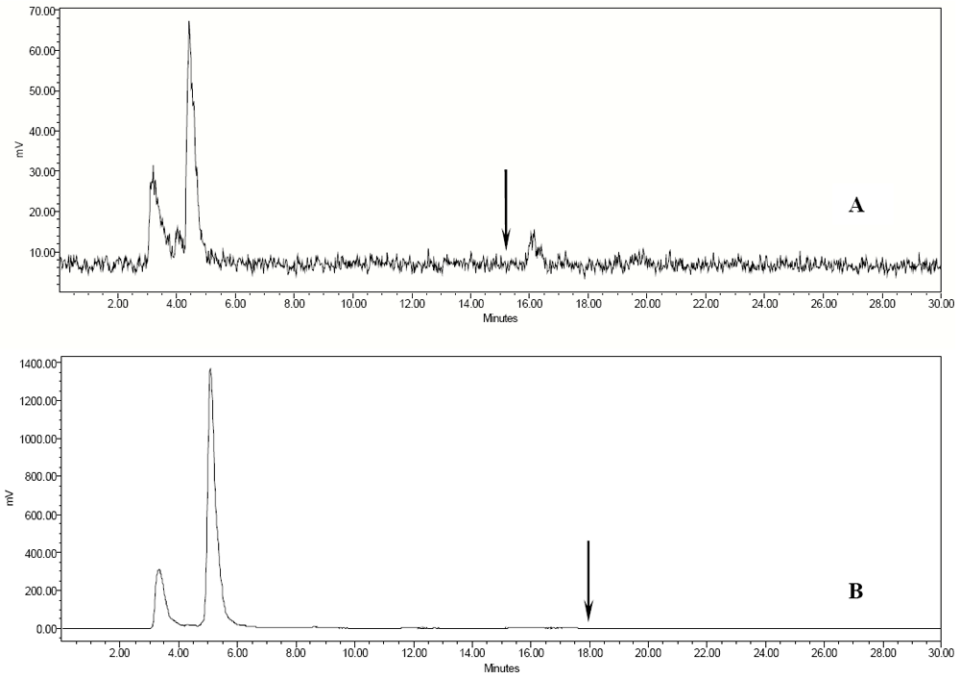

Figure 6.

HPLC profiles of radioactive urine samples of B16/F1 murine melanoma-bearing C57 mice at 2 h post-injection of ^{111}In-DOTA-CycMSH (A) and ^{111}In-DOTA-GlyGlu-CycMSH (B). Arrows indicate retention time of the original compound of ^{111}In-DOTA-CycMSH and ^{111}In-DOTA-GlyGlu-CycMSH prior to the tail vein injection.

Table 1

Biodistribution of ^{111}In-DOTA-Cyc(Arg^{11})CCMSH and ^{111}In-DOTA-GlyGlu-Cyc(Arg^{11})CCMSH in B16/F1 murine melanoma-bearing C57 mice. The data were presented as percent injected dose/gram or as percent injected dose (Mean±SD, n=5).

	Percent injected dose/gram (%ID/g)							
	^{111}In-DOTA-CycMSH				^{111}In-DOTA-GlyGlu-CycMSH			
Tissues	**2 h**	**2 h blockade**	**4 h**	**24 h**	**2 h**	**2 h blockade**	**4 h**	**24 h**
Tumor	9.53±1.41	0.29±0.14	7.54±0.70	2.22±0.51	10.40±1.40	0.27±0.10	7.40±0.43	2.37±0.28
Brain	0.06±0.02	0.05±0.04	0.05±0.04	0.02±0.03	0.10±0.07	0.01±0.02	0.02±0.03	0.05±0.04
Blood	0.09±0.14	0.11±0.11	0.01±0.00	0.05±0.06	0.14±0.05	0.12±0.11	0.02±0.04	0.09±0.14
Heart	0.20±0.18	0.17±0.15	0.06±0.05	0.07±0.13	0.16±0.18	0.04±0.06	0.00±0.00	0.09±0.17
Lung	0.22±0.18	0.10±0.10	0.11±0.10	0.03±0.06	0.04±0.03	0.12±0.14	0.01±0.00	0.06±0.05
Liver	0.17±0.03 *	0.12±0.00	0.09±0.07 *	0.11±0.01 *	0.27±0.03	0.25±0.05	0.21±0.02	0.24±0.08
Spleen	0.39±0.41	0.42±0.37	0.80±0.39	0.22±0.39	0.16±0.33	0.15±0.14	0.27±0.40	0.15±0.25
Stomach	0.10±0.06	0.08±0.10	0.13±0.15	0.02±0.04	0.06±0.07	0.03±0.05	0.02±0.03	0.04±0.07
Kidneys	16.16±1.86 *	16.21±2.33	21.69±0.34 *	16.00±2.30 *	13.07±2.49	8.61±1.34	12.13±1.17	9.06±1.82
Muscle	0.14±0.10	0.28±0.32	0.01±0.01	0.03±0.04	0.06±0.12	0.13±0.13	0.05±0.06	0.05±0.06
Pancreas	0.07±0.06	0.13±0.04	0.03±0.05	0.07±0.06	0.07±0.10	0.09±0.15	0.05±0.08	0.02±0.02
Bone	0.20±0.16	0.16±0.14	0.04±0.05	0.18±0.13	0.14±0.07	0.42±0.37	0.00±0.00	0.06±0.05
	Percent injected dose (%ID)							
Intestines	0.34±0.11	0.23±0.06	0.25±0.08	0.05±0.02	0.27±0.15	0.27±0.06	0.15±0.01	0.07±0.02
Urine	91.70±0.62	94.53±0.65	92.34±0.80	94.69±0.49	90.32±1.64	96.52±0.20	92.36±0.74	95.04±0.84
	Uptake ratio of tumor/normal tissue							
Tumor/Blood	105.89	2.64	754.00	44.40	74.29	2.25	370.00	26.33
Tumor/Kidneys	0.59	0.02	0.35	0.14	0.80	0.0.3	0.61	0.26
Tumor/Lung	43.32	2.90	68.55	74.00	260.00	2.25	740.00	39.50
Tumor/Liver	56.06	2.42	83.78	20.18	38.52	1.08	35.24	9.88
Tumor/Muscle	68.07	1.04	754.00	74.00	173.33	2.08	148.00	47.40

* $P<0.05$, significance comparison between ^{111}In-DOTA-CycMSH and ^{111}In-DOTA-GlyGlu-CycMSH at 2, 4 and 24 h post-injection.